BIOCHEMISTRY
including biophysical chemistry & molecular biology

Article

pubs.acs.org/biochemistry

DNA-Mediated Oxidation of p53

Kathryn N. Schaefer and Jacqueline K. Barton*

Division of Chemistry and Chemical Engineering, California Institute of Technology, Pasadena, California 91125, United States

Supporting Information

ABSTRACT: Transcription factor p53 is the most commonly altered gene in human cancer. As a redox-active protein in direct contact with DNA, p53 can directly sense oxidative stress through DNA-mediated charge transport. Electron hole transport occurs over long distances through the π-stacked bases and leads to the oxidative dissociation of p53. The extent of protein dissociation depends upon the redox potential of the DNA in direct contact with each p53 monomer. The DNA sequence dependence of p53 oxidative dissociation was examined by electrophoretic mobility shift assays using oligonucleotides containing both synthetic and human p53 consensus sequences with an appended photooxidant, anthraquinone. Greater p53 dissociation is observed from sequences containing low-redox potential purine regions, particularly guanine triplets. Using denaturing polyacrylamide gel electrophoresis of irradiated anthraquinone-modified DNA, the DNA damage sites corresponding to sites of preferred electron hole localization were determined. The resulting DNA damage preferentially localizes to guanine doublets and triplets. Oxidative DNA damage is inhibited in the presence of p53, but only at sites in direct contact with p53. From these data, predictions about the sensitivity of human p53-binding sites to oxidative stress as well as possible biological implications have been made. On the basis of our data, the guanine pattern within the purine region of each p53-binding site determines the response of p53 to DNA oxidation, yielding for some sequences the oxidative dissociation of p53 from a distance and thereby providing another potential role for DNA charge transport chemistry within the cell.

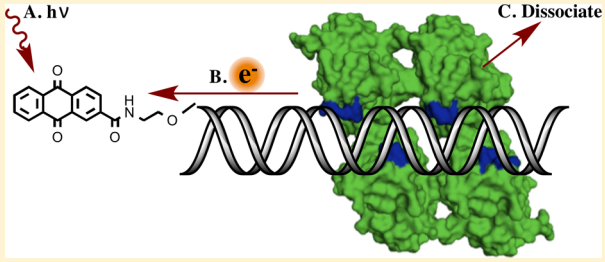

Human transcription factor p53 transduces a variety of cellular stresses into transcriptional responses. The pivotal role that p53 plays in human cells classifies this protein as a tumor suppressor. Many of the pathways in which p53 is involved revolve around decisions of cellular fate, including responses like apoptosis, senescence, cell cycle arrest, or DNA repair.[1−6] The importance of p53 integrity for proper biological function is highlighted by the fact that mutations in this protein are observed in more than half of all human cancers, with the majority of these mutations occurring within the DNA-binding domain.[7,8] Such mutations may cause improper protein folding, disruption of integral protein−protein interactions, or alteration of protein−DNA contacts.[7] While p53 is generally known to sense oxidative stress as one of its inputs, its function as a redox-active DNA-binding protein remains to be fully elucidated. Here we focus on a new mechanism by which p53 may directly sense and respond to oxidative stress within the genome.

Our laboratory has focused on studies of long-range charge transport (CT) through DNA. We have found that oxidative damage to DNA can occur from a distance because of the migration of electron holes through the DNA base stack.[9−12] Perturbations in the intervening base pair stack, such as abasic sites and base mismatches, severely attenuate DNA CT.[12−14] We have exploited this property in electronic devices to detect base mismatches and base lesions and to characterize DNA-binding proteins.[13−15] By using a variety of distally bound photooxidants, we have also measured effective CT through DNA over a distance of 34 nm; much longer distances for CT are expected given the very weak distance dependence observed.[12,16,17] Inside the cell, possible sources of DNA oxidation include ionizing radiation, exogenous chemicals, and metabolic side products. Given the ease of electron hole migration through DNA, we expect holes to localize to DNA sites with the lowest redox potential, particularly guanine doublets and triplets.[18] Oxidation of the 5′ G in guanine doublets and triplets has become a hallmark of one-electron oxidation of DNA. Guanine radicals can yield a myriad of mutagenic lesions as a result of reacting with water or dioxygen.[19] Bound proteins may also react with the base radicals to form covalent adducts.[20] While most studies have characterized this chemistry using synthetic oligonucleotides *in vitro*, we have also seen that long-range oxidative damage can occur in chromatin as well as in the nucleus of HeLa cells.[21−23]

We have proposed a model whereby DNA CT plays an integral biological role in DNA damage sensing as a first step in DNA repair.[24] DNA CT is a first step in the search for DNA base lesions, given the prevalence of 4Fe−4S clusters in base excision repair enzymes. More recently, 4Fe−4S clusters have been found in the full range of DNA-processing enzymes, suggesting a general role for DNA CT within the cell in long-range signaling of genomic integrity.[10,24] DNA CT recognition

Received: March 13, 2014
Revised: May 9, 2014
Published: May 22, 2014

   dx.doi.org/10.1021/bi5003184 | *Biochemistry* 2014, 53, 3467−3475

by proteins does not necessarily require an iron−sulfur cluster; other redox-active moieties within a protein can participate, as well. Cysteine residues can be oxidized to form disulfides at physiological redox potentials. As shown electrochemically and by photooxidation, thiols incorporated into the DNA backbone can be oxidized to disulfides at a distance through long-range DNA CT.[25,26] Cysteine redox chemistry is often harnessed *in vivo* by DNA-bound proteins as a redox switch in regulation; DNA CT chemistry would offer the ability to conduct such reactions from a distance.

Redox activation in proteins through thiol switches by long-range DNA CT was investigated by focusing on p53. The DNA-binding domain of p53 contains 10 cysteine residues, most of which are well-conserved. Three of these residues coordinate a zinc ion, while the rest may play a role in coupling to DNA, oxidation, and terminal disulfide formation.[27−29] Electromobility shift assays were first used to determine that p53 can be oxidized through DNA from a distance using a tethered DNA photooxidant, while mass spectrometry results suggested the concurrent formation of a disulfide.[28] Curiously, DNA-mediated oxidation and dissociation of p53 were seen with p53 bound to the *Gadd45* promoter but not from the *p21* promoter, though reduced affinities of p53 for these promoter sites were comparable. This sequence selectivity in DNA-mediated oxidation of p53 indicates an element of control was possible, where binding to some promoter sites would lead to oxidative modification but not to others. Interestingly, this sequence selectivity with regard to oxidation correlates with the biological regulation of p53 under conditions of oxidative stress.

Here we explore the role that DNA sequence plays in p53 oxidation in greater detail. Our first goal is to understand the basis for the sequence selectivity associated with oxidative dissociation. We then explore how sequence context may play a role in p53 regulation more generally to determine if this mechanism may represent a means of controlling p53 activity within the cell under oxidative stress.

MATERIALS AND METHODS

Oligonucleotide Synthesis and Purification. Oligonucleotides were synthesized on an ABI 3400 DNA synthesizer using standard phosphoramidite chemistry. Sequences not containing anthraquinone (AQ) were synthesized with the dimethoxytrityl (DMT) group intact. Cleavage from the resin and deprotection were conducted by incubation in NH_4OH overnight at 60 °C and dried *in vacuo*. The oligonucleotides were purified by reversed phase C-18 high-performance liquid chromatography (HPLC) (2 to 32% acetonitrile against 50 mM ammonium acetate over 30 min). DMT removal was conducted by a 15 min incubation in 80% acetic acid and quenched by 200 proof ethanol and 3 M sodium acetate. Once dry, the oligonucleotides were subjected to a second round of reversed phase HPLC (2 to 17% acetonitrile against 50 mM NH_4OAc over 30 min). Oligonucleotides for the AQ photooxidant-tethered stands were synthesized with the DMT group removed. An AQ derivative, carboxylic acid(2-hydroxyethyl)amide, was converted to its respective phosphoramidite and incorporated onto the 5′ end of the sequence through a 15 min coupling on the ABI 3400 DNA synthesizer.[30,31] AQ-conjugated oligonucleotides were cleaved from the resin and deprotected as previously described. AQ-DNA was purified by one round of reversed phase HPLC (2 to 17% acetonitrile against 50 mM NH_4OAc over 30 min). Oligonucleotides were column desalted (Sep-pak, Millipore), characterized by matrix-assisted laser desorption ionization time-of-flight mass spectrometry (Applied Biosystems Voyager DE-PRO), and quantified by UV−visible spectroscopy (Beckman DU7400 spectrophotometer) at their respective ε_{260} values. We formed double-stranded oligonucleotides by annealing equimolar amounts of complementary single strands by heating them at 90 °C for 5 min and cooling them to ambient temperature in 5 mM potassium phosphate and 50 mM NaCl (pH 7.5).

Protein Production. The p53′ protein used is a full-length human p53 containing three stabilizing mutations: M133L, V203A, and N268D.[32] The gene for p53′ was cloned from the quadruple mutant p53 plasmid N239Y/M133L/V203A/N268D.[32] Polymerase chain reaction mutagenesis by overlap extension and gene splicing were used to restore N239, and the sequence was verified by Laragen.[33] The p53′ protein was overexpressed and purified as described previously.[34] Dithiothreitol was diluted to nanomolar levels with p53 buffer [20 mM Tris, 100 mM KCl, 0.2 mM EDTA, and 20% glycerol (pH 8.0)] before the protein was flash-frozen and stored at −80 °C.

5′ Oligonucleotide Radiolabeling. Single-stranded oligonucleotides were 5′ labeled with [γ-^{32}P]dATP (PerkinElmer) as described previously.[35] The purified samples were dried *in vacuo* and resuspended in 5 mM potassium phosphate and 50 mM NaCl (pH 7.5).

3′ Oligonucleotide Radiolabeling. The 3′ radiolabeling was conducted for DNA strands conjugated with anthraquinone at the 5′ end. The AQ oligonucleotides were radiolabeled using [γ-^{32}P]dTTP (MP Biomedicals) and Terminal Transferase (New England Biolabs). The samples were mixed under standard NEB protocol conditions, incubated for 2 h at 37 °C, and subsequently passed through two Micro Bio-Spin 6 columns at 3000 rpm. Samples were purified as described previously.[39]

Electrophoretic Mobility Shift Assay of p53′. p53′ protein was allowed to bind to the radiolabeled oligonucleotides with a 1:1 DNA:protein tetramer ratio (100 nM 1% 5′-radiolabeled duplex and 400 nM p53 monomer) in the presence of 5 μM dAdT competitor DNA (IDT), 0.1% NP-40 (Surfact-Amps NP-40, Thermo Scientific), 0.1 mg/mL BSA in 20 mM Tris-HCl (pH 8.0), 20% glycerol, 100 mM KCl, and 0.2 mM EDTA. The concentration of p53′ used was dependent upon the K_D of the protein for the natural consensus sequences, to ensure a minimum of 80% DNA bound with p53. Samples were made at 4 °C and irradiated on ice for varying lengths of time using a solar simulator (ORIEL Instruments) utilizing a UVB/UVC long-pass filter to avoid direct DNA strand damage. The radioactivity of each sample was determined by scintillation counting (Beckman LS 5000TD) and normalized prior to the samples being loaded onto a 10% TBE polyacrylamide gel (Bio-Rad). Each gel was run in 0.5× TBE buffer at 4 °C and 50 V for 1.5 h. DNA from the gel was transferred to Amersham Hybond-N nucleotide blotting paper (GE Healthcare) with a semidry electroblotter (Owl HEP-1) for 1 h at 175 mA in transfer buffer [25 mM Tris-HCl, 200 mM glycine, and 10% methanol (pH 8.5)]. The blots were exposed to a phosphorimaging screen (GE Healthcare), imaged with a STORM 820 scanning system (Molecular Dynamics), and analyzed using Image Quant, Excel, and Oracle. All data were normalized to the corresponding unirradiated control. The change in p53 binding was determined by monitoring the free DNA signal over the total DNA signal in each lane.

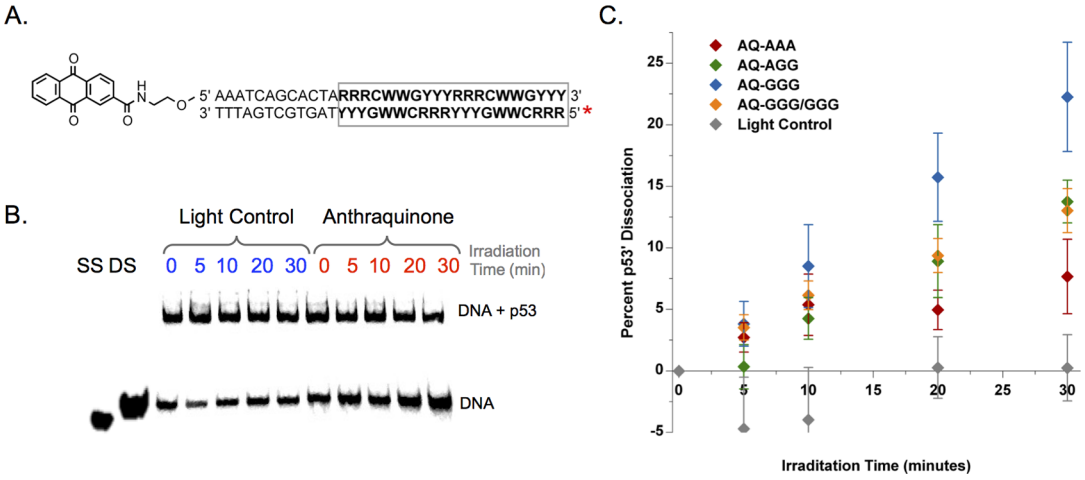

Figure 1. Oxidative dissociation of p53 from sequences with varied oxidation potentials. (A) DNA-mediated oxidation of p53 is induced by irradiation of an appended anthraquinone photooxidant. The consensus site for p53 is boxed, and the red asterisk denotes the location of the ^{32}P label. (B) Representative autoradiogram of a p53′ electromobility gel shift assay using the unnatural GGG sequence. Light control samples do not have an anthraquinone photooxidant conjugated to the DNA, and the overall amount of DNA-bound p53′ changes minimally. The anthraquinone samples contain the appended photooxidant, and an increase in the amount of lower-molecular weight free DNA is observed with an increased level of irradiation. (C) Plot quantifying the percent change in p53′–DNA binding with respect to irradiation time for the four different synthetic consensus sequences compared to the LC. Sequence constructs are listed in Table 1. The percent change in p53′ binding is determined as the free DNA signal over the total lane signal, normalized to the unirradiated control. Error bars reflect the standard error of the mean over a minimum of three replicates. Samples contained 100 nM duplex, 400 nM p53′ monomer, 5 μM dAdT, 0.1% NP-40, 0.1 mg/mL BSA in 20 mM Tris-HCl (pH 8.0), 20% glycerol, 100 mM KCl, and 0.2 mM EDTA.

Table 1. p53 Consensus Sequence Oligonucleotides

construct name	DNA sequence (5′–3′)[a]	K_D (nM)[b]	GC %[c]	GG[d]	GGG[e]
AAA	AAATCAGCACTAAAACATGTCTAAACATGTCT	230 ± 40	30.0	–	–
AGG	AAATCAGCACTAAGGCATGTCTAGGCATGTCT	430 ± 110	50.0	2	–
GGG	AAATCAGCACTAGGGCATGTCTGGGCATGTCT	360 ± 70	60.0	–	2
GGG/GGG	AAATCAGCACTAGGGCATGCCCGGGCATGCCC	220 ± 40	80.0	–	4
Caspase	AAATCAGCACTAATAAAGACATGCATATGCATGCACA	610 ± 80	36.0	–	–
S100A2	AAATCAGCACTAGGGCATGTGTGGGCACGTTC	330 ± 20	65.0	–	2

[a]Locations of altered purine nucleobases in direct p53 contact are underlined in the synthetic constructs. [b]The apparent K_D of p53′ (in monomer units) was determined at 100 nM duplex, 5 μM dAdT, 0.1% NP-40, 0.1 mg/mL BSA in 20 mM Tris-HCl (pH 8.0), 20% glycerol, 100 mM KCl, and 0.2 mM EDTA at 4 °C and the sample electrophoresed at 50 V on a 10% polyacrylamide gel in 0.5× TBE. A representative autoradiogram is given in Figure S1 of the Supporting Information. [c]GC % of the consensus sequence, not including the 5′ linker. [d]Number of guanine doublets within the consensus site. [e]Number of guanine triplets within the consensus site.

Assay of Oxidative DNA Damage. Samples were prepared from a stock solution containing 1 μM 100% 3′ ^{32}P-labeled oligomer duplex, 5 μM dAdT competitor DNA, 0.1% NP-40, and 0.1 mg/mL BSA in p53 buffer [20 mM Tris-HCl, 100 mM KCl, 0.2 mM EDTA, and 20% glycerol (pH 8.0)]. The p53′ concentrations ranged from 0 to 40 μM. DNA damage was induced by irradiation for 1 h using a solar simulator with a UVB/UVC long-pass filter. Irradiated samples were treated with a 10% piperidine solution with 0.2 unit of calf thymus DNA and heated at 90 °C for 30 min to cleave damaged sites. Excess piperidine was removed by drying samples *in vacuo*. DNA was ethanol precipitated to ensure purity. The dry samples were resuspended in denaturing formamide loading buffer and heated for 2 min at 90 °C, and equivalent levels of radioactivity were loaded per lane onto a prerun 20% polyacrylamide gel and run at 90 W for 3 h in 1× TBE buffer. Sequencing lanes were created by standard Maxam–Gilbert sequencing reactions.[36] Gels were visualized by phosphorimagery and quantified using ImageQuant and Excel.

RESULTS

p53′–DNA Electromobility Gel Shift Assays with Synthetic p53 Consensus Sequences. The protein used in all of the following experiments is a full-length human p53 containing three thermodynamically stabilizing mutations: M133L, V203A, and N268D.[32] These mutations do not lead to differences in DNA binding affinity or oxidative dissociation compared to those of the wild-type protein but result in a far more robust and stable protein for experimentation. This mutant protein is designated as p53′. Four synthetic DNA consensus sequences were constructed and used for *in vitro* experiments to determine the influence of the guanine pattern in allowing oxidative dissociation of DNA-bound p53′ by DNA CT. The oligonucleotides were designed to contain the canonical p53 consensus sequence pattern composed of two response elements with no space between them, 5′-RRRCW-WGYYY-3′, with R representing a purine, Y representing a pyrimidine, and W being either an adenine or a thymine.[37] As seen in Figure 1, the consensus site is flanked 5′ with a 12-nucleotide linker to which an anthraquinone photooxidant

dx.doi.org/10.1021/bi5003184 | *Biochemistry* 2014, 53, 3467–3475

(AQ) is covalently bound. A ^{32}P radiolabel is located on the 5′ end of the complementary strand for visualization.

Photooxidation of p53′ induces a change in protein affinity and can promote its dissociation from DNA, which we can observe using a gel shift assay. The purine contents of the four synthetic consensus sequences range from no sequential guanine bases to four sets of guanine triplets, all while fully conforming to consensus sequence constraints. The relative reactivity of bases to one-electron oxidation varies as follows: 5′-GGG > 5′-GG > 5′-GA > 5′-AA.[18,38] The relative reactivity directly correlates with the calculated ionization potentials of stacked bases; the lower the ionization potential, the greater the observed relative reactivity.[38] Dissociation constants for the dissociation of p53′ from the oligonucleotides lacking AQ are listed in Table 1. The change in p53′ binding upon DNA photooxidation is determined as the fraction of free DNA signal over total DNA signal per lane normalized to its respective unirradiated control, with error bars reflecting the standard error of the mean obtained over a minimum of three trials. All samples contained 100 nM consensus sequence DNA and 400 nM p53′ to ensure a 1:1 DNA:p53′ tetramer ratio.

It should be noted that we determined earlier that this oxidative dissociation of p53 was found to be the result of oxidation from a distance through DNA CT.[28] Intervening mismatches between the AQ and p53-binding site inhibit p53 dissociation because those intervening mismatches inhibit DNA CT. Mass spectrometry studies furthermore show that protein oxidation is associated with disulfide bond formation (unpublished results in our laboratory).[28]

The degree of p53′ oxidative dissociation is found to vary according to the sequence of the oligonucleotide and is dependent upon photoexcited anthraquinone (Figure 2). All constructs of light control DNA strands (LC), which are irradiated but do not contain an appended anthraquinone for oxidation, display negligible dissociation of p53′. Dissociation from all of the sequences is relatively linear with respect to irradiation time, with maximal dissociation of p53′ observed after 30 min. A longer irradiation past 30 min did not significantly increase the overall level of p53 oxidative dissociation. The AQ-AAA sequence confers the least overall oxidatively induced dissociation of p53′ with a maximal dissociation of 7.7%.

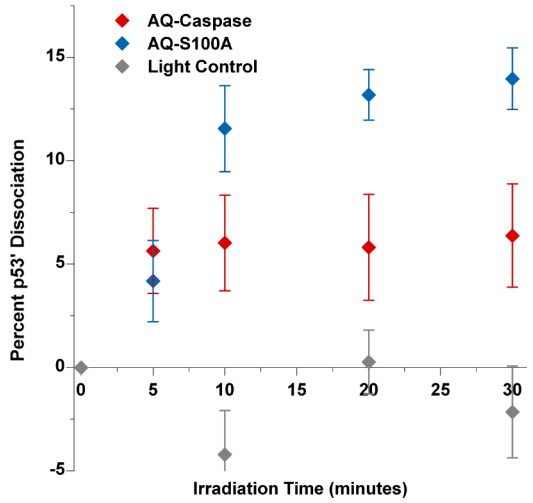

Figure 2. Oxidative dissociation of p53 from human promoter sequences. Plot quantifying the percent change in three types of p53–DNA binding with respect to irradiation time for the natural human p53 consensus sequences Caspase and S100A. Sequence constructs are listed in Table 1. The fraction of p53′ dissociation was determined as the ratio of the percent of bound DNA in the irradiated sample to that in the dark control. Error bars reflect the standard error of the mean obtained from a minimum of four trials. Samples contained 100 nM duplex, 500 nM p53 monomer for S100A2 and 800 nM p53 monomer for Caspase, 5 μM dAdT, 0.1% NP-40, 0.1 mg/mL BSA in 20 mM Tris-HCl (pH 8), 20% glycerol, 100 mM KCl, and 0.2 mM EDTA.

The AQ-AGG and AQ-GGG/GGG sequences both display similar extents of dissociation with maxima of 13.8 and 13.0%, respectively. The DNA sequence that displayed the greatest amount of p53′ dissociation is AQ-GGG (22.3%). Thus, the highest levels of DNA CT oxidative dissociation of p53′ were observed from consensus sequences with low-redox potential guanine doublets and triplets.

p53′–DNA Electromobility Shift Assays with Human p53 Promoter Sequences. To determine whether the gel shift results obtained from the synthetic sequences can be applied to human p53 response elements, two naturally occurring human p53 response elements were also investigated: Caspase1A (Caspase) and S100 calcium-binding protein A2 (S100A). DNA sequence constructs using their respective response elements and their relative dissociation constants are also listed in Table 1. Caspase1A is a cysteine-dependent aspartate-directed protease and plays essential roles in apoptosis, necrosis, and inflammation.[39] This human p53 response element promotes the production of caspase when p53 is bound. The response element of Caspase1A is similar to the synthetic AAA sequence, with an adenine triplet within the purine region of the consensus sequence and no guanine doublets or triplets in either of the complementary strands.[39] Conversely, the S100A2 protein is intimately involved in cell cycle progression and cellular differentiation and may function as a tumor suppressor.[40,41] When p53 is bound to this guanine-rich sequence, production of the S100A2 protein is promoted. The S100A2 response element is very similar to the synthetic GGG sequence, containing two guanine triplets within the purine regions. The human response elements were constructed in the same manner as the synthetic sequences described above with an appended 5′-anthraquinone photooxidant, the same 12-nucleotide linker, and the complementary strand labeled with 5′ [^{32}P]ATP. The relative dissociation constant (K_D) for p53 with each sequence was determined by a gel shift assay and quantified with ImageQuant and Excel.

Experiments were conducted at the protein concentration at which 80% of the radiolabeled oligonucleotides were bound with p53′, based upon their respective K_D values, 500 nM for the S100A sequence and 800 nM for the Caspase sequence. The AQ-S100A sequence with two guanine triplets yields a significantly greater level of oxidative dissociation of bound p53′ (14.0%), while the AQ-Caspase sequence yields a maximum of 6.4% dissociation. These sequences do not oxidize p53 linearly with irradiation, instead leveling out at earlier irradiation time points. This difference likely is related to the higher concentration of p53′ used and the possibility of re-equilibration of reduced p53′ with dissociated DNA.

Comparison between Natural and Synthetic p53 Consensus Sequences. Figure 3 shows the direct comparison between synthetic and natural human sequences. We find that synthetic and natural consensus sequences with varied oxidation potentials due to altered purine patterns within the p53 consensus sequence exhibit the following trend in terms of

dx.doi.org/10.1021/bi5003184 | Biochemistry 2014, 53, 3467–3475

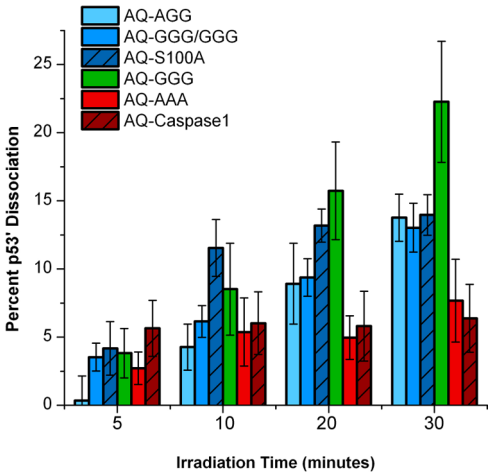

Figure 3. Comparison of natural and unnatural p53 consensus sequences via EMSA. On the right (red), AQ-Caspase and AQ-AAA display minimal oxidative dissociation even at long irradiation times. The sequences that allow for oxidative dissociation of p53′, AQ-S100A2, AQ-AGG, and AQ-GGG/GGG, are compared on the left (blue). AQ-GGG (green) displays the strongest oxidative dissociation of p53′.

increasing levels of p53 oxidation: AQ-AAA, AQ-Caspase (red) < AQ-GGA, AQ-GGG/GGG, AQ-S100A (blue) < AQ-GGG (green).

The AQ-Caspase sequence displays minimal dissociation of p53′ upon photooxidation, comparable to that seen with the synthetic AQ-AAA sequence. The high-redox potential adenine triplet within the purine region does not allow for facile transfer of an electron hole from the DNA to the bound p53′. The AQ-S100A sequence, in contrast, displays high levels of oxidative dissociation upon irradiation, similar to the AQ-AGG and AQ-GGG/GGG synthetic sequences after irradiation for 30 min. Therefore, even with different sequences, the guanine pattern within the purine region of the consensus sequence allows for equivalent oxidative dissociation of p53′ with equivalent amounts of irradiation.

Long-Range Oxidative Damage with and without p53′ Examined with Denaturing Polyacrylamide Gels. To determine the exact locations within the synthetic oligonucleotides to which the electron holes localize, denaturing polyacrylamide gels were utilized to determine sites of oxidative DNA damage. The oligonucleotides were radiolabeled with ^{32}P at the 3′ end for visualization and treated with piperidine to cleave the DNA backbone at the site of oxidative damage.[36] When compared to Maxam−Gilbert sequencing lanes and the unirradiated control, the locations of DNA oxidative damage induced by photooxidation are observed as distinct bands on the denaturing polyacrylamide gel. Representative gels for each synthetic sequence are included in Figure S2 of the Supporting Information. The intensity of each piperidine cleavage site is measured in comparison to the total signal intensity of the entire lane. Protein p53′ was also titrated into the samples to assess how the protein inhibits DNA damage. The presence of p53′ inhibits DNA damage via the transfer of the electron hole from the DNA to the protein, as shown in Figure 4.

Oxidative damage is apparent primarily at the 5′ G of guanine doublets and triplets, as expected. After irradiation for 1 h of the AQ-AAA sequence, which lacks guanine repeats, oxidative damage is observed only at the single 5′ G near the

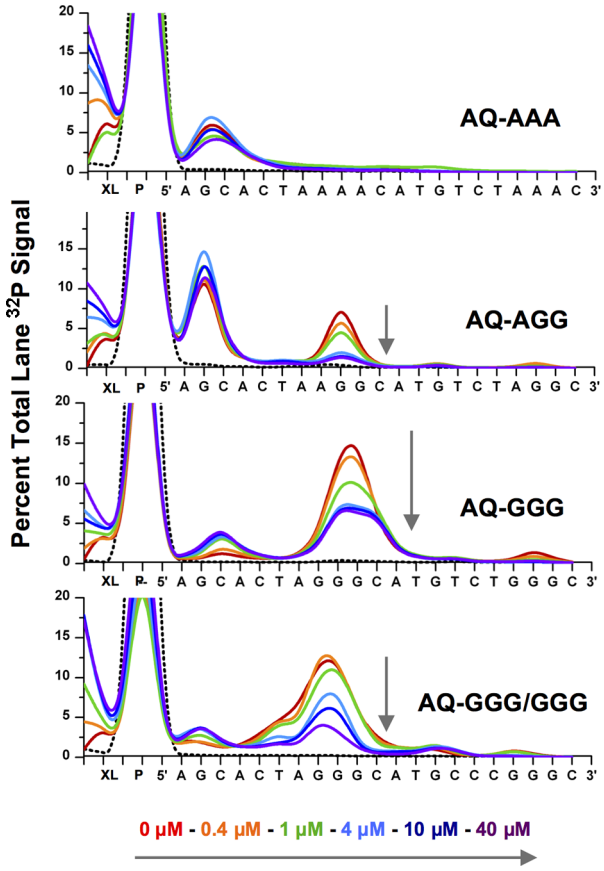

Figure 4. Guanine oxidation assays. Representative guanine oxidation gel shift assays of the four 3′-radiolabeled synthetic consensus sequences displaying lane profiles at varying protein concentrations. The gels were analyzed using Imagequant, and each band was calculated as the percent of the total lane signal. The dotted black line represents the unirradiated control. The concentration of p53′ in the irradiated samples is varied from 0 μM (red) to 40 μM (purple). Samples contained 1 μM AQ-Duplex, 5 μM dAdT, 0.1% NP-40, 0.1 mg/mL BSA in 20 mM Tris-HCl (pH 8), 20% glycerol, 100 mM KCl, and 0.2 mM EDTA.

tethered oxidant; this guanine is not contained within the consensus sequence. Additionally, this damage is not inhibited upon addition of p53′. The AQ-AGG sequence displays damage within the consensus sequence primarily at the 5′-GG location and at the single guanine located in the linker region, adjacent to the oxidant. Upon the addition of a 10-fold excess of p53′ tetramer, a full recovery of the damage within the consensus sequence guanine doublet is observed. In contrast, no recovery is observed at the single guanine in the linker region. Sequences AQ-GGG and AQ-GGG/GGG both displayed the majority of their oxidatively induced damage at the 5′-guanine triplet site within the consensus sequence region, with no significant damage in the linker region. The addition of p53′ to both AQ-GGG and AQ-GGG/GGG mitigates DNA base damage within the consensus sequence. In these sequences, the damage is not fully quenched by p53′ concentrations of up to 40 μM.

Damage was not readily observed at the purine regions near the 3′ end. Ethanol precipitation of the samples may have led to the loss of these low-molecular weight products. In all of the sequences, some higher-molecular weight products are also observed and can be attributed to the formation of covalently

dx.doi.org/10.1021/bi5003184 | *Biochemistry* 2014, 53, 3467−3475

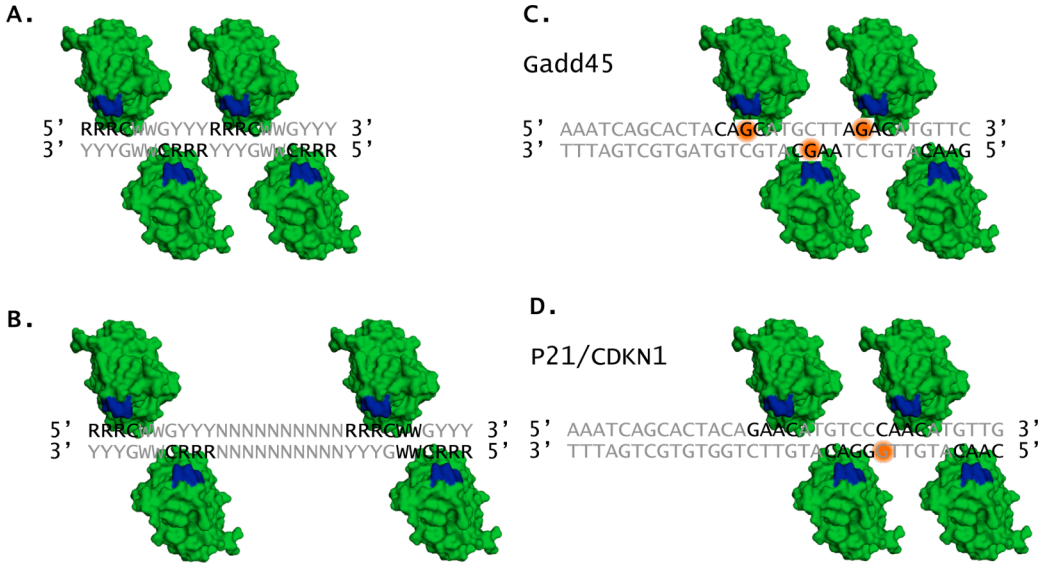

Figure 5. Consensus sequence–p53 interaction. All diagrams are representations modeled from the 3KMD crystal structure by Chen et al.[23] (A) p53 tetramer (green) bound to a canonical consensus sequence. The contacting p53 residues are colored blue and the nucleobases to which they hydrogen bond black. (B) Representation of a p53 tetramer bound to a consensus site with a 10-nucleobase linker between the two half-sites. (C) Representative binding of a p53 tetramer to the Gadd45 consensus site. The orange circles indicate anticipated locations at which an electron hole localizes within direct contact of a p53 monomer. (D) Representative binding of a p53 tetramer to the p21 consensus site. The expected location of electron hole localization in denoted by the orange circle and is between the two half-sites and not in direct contact with p53.

cross-linked products. Irradiation without the addition of p53′ gives one band that is indicative of a cross-link between the two DNA strands. The higher-molecular weight bands are indicative of possible p53–DNA cross-links.

DISCUSSION

Sequence Dependence of p53′ Dissociation. Electron holes in DNA localize to regions of low redox potential, most notably guanine doublets and triplets. Specific sequences of oligonucleotides incorporating guanine doublets and triplets into the purine regions of the consensus site permitted the study of how the guanine pattern in p53 consensus binding sites influences oxidative dissociation of p53. Sequences containing low-redox potential guanine doublets and triplets allow oxidative dissociation of p53′; we refer to these as responsive sequences. Figure 1 shows maximal dissociation of p53′ from the responsive sequences of AQ-GGG at 22.3%, followed by AQ-AGG, and AQ-GGG/GGG around 13.0%. The AQ-AAA sequence confers minimal p53′ dissociation (7.7%), and we categorize this as a nonresponsive sequence.

Electron hole occupancy at a particular location can be described in the context of overall residence times. Upon equilibration along the DNA base stack, an electron hole spends more time on a low-redox potential GGG site rather than a high-redox potential AAA site. The finding that the AQ-GGG/GGG sequence did not yield the most oxidative dissociation of p53′ is noteworthy. In the double-stranded promoter site, the AQ-GGG sequence has two locations in which holes can reside, while the AQ-GGG/GGG has four. Effectively, the electron hole density in each GGG site of AQ-GGG/GGG is half of that of AQ-GGG, resulting in approximately half the p53′ dissociation of AQ-GGG.

Importantly, the locations of low-redox potential sites should align with the p53–DNA major groove interface to allow effective protein–DNA electron transfer. Thus, not all low-potential sites within a consensus sequence are expected to transfer an electron hole to p53′, only those in close contact with the protein. CT in proteins decays exponentially with distance, highlighting the necessity for low-redox potential bases at the DNA–p53 interface for this process to occur. The denaturing DNA damage gels of Figure 4 illustrate the necessity both of proper p53 contact for electron hole transfer and of the redox potentials of purines in contact with p53 for conferring a sensitive response. As highlighted in the AQ-AAA and AQ-AGG sequences, damage does occur at the guanine in the linker region, but that damage is not inhibited by p53′. The inhibition of damage with protein binding is seen only at those sites in contact with p53′. Moreover, for oxidative dissociation of p53 to occur, the bases in contact with p53′ must be able to initially trap the electron hole with an overall low redox potential. Thus, the hole localization within the consensus sequence ultimately dictates the responsiveness of the site to oxidative dissociation.

To establish whether natural p53-binding sites respond similarly to the synthetic ones, two sequences were studied. The natural sequences were found to behave like their synthetic counterparts because of similar guanine patterns in the purine region of the consensus site. Upon oxidation, p53′ dissociates from S100A2, which is similar to the responsive synthetic sequences due to the presence of two guanine triplets; S100A2 is thus classified as a responsive sequence. Because p53 promotes S100A2 expression when bound, oxidative stress would lead to p53 dissociation and downregulation of the gene, resulting in diminished tumor suppressor activity. In contrast, the Caspase sequence is similar to the AQ-AAA synthetic sequence. Minimal dissociation of p53′ from Caspase is observed, designating the Caspase p53-binding sequence as nonresponsive. Thus, upon oxidation, p53 would be expected to remain mostly bound, leading to the continued promotion of Caspase. The continual promotion of Caspase production by p53 during times of oxidative genomic stress signals the cell to continue toward apoptosis.

dx.doi.org/10.1021/bi5003184 | *Biochemistry* 2014, 53, 3467–3475

Making Predictions about Natural p53 Promoter Sequences with Oxidative Stress. We can also compare these results to those of our earlier work that demonstrated a contrasting oxidation response in p53 between recognition elements corresponding to Gadd45 (DNA repair) and p21 (cell cycle arrest), now known as CDKN1A.[28] These p53-binding sites contain identical G/C percentages but display different guanine patterns overall. The p53-bound Gadd45 sequence can be classified as responsive, yielding oxidative dissociation of p53. In contrast, little p53 oxidation was seen from the p21 sequence, leading to this site being characterized as nonresponsive. Figure 5 highlights the p53 residues that nest in the major groove [K120, S121, C277, and R280 (blue)] and the bases of the consensus sequence with which they directly interact (black). As a general example, Figure 5A depicts two half-sites with no intervening spacer base pairs, highlighting the importance of low-redox potential guanines at the 5′-RRRG-3′ site in direct contact with p53 for responsiveness. The p53 consensus site is known to contain a 0−13 bp linker region between the two p53 half-sites; certain p53-binding sites may conform to consensus constraints but contain low-redox potential sites that are not in direct contact with p53. Figure 5B depicts p53 binding to a consensus site with a 10-base linker between the two half-sites. Guanine triplets located within this linker region would be favorable locations for electron hole localization; however, the electron holes would be funneled away from the direct p53 contact sites, and the overall responsiveness of that site would decrease. The recognition sequence for Gadd45 is shown to be responsive by a gel shift assay. Figure 5C illustrates that the p53 consensus site for Gadd45 indeed has guanines directly aligned with the p53 contact residues, and these guanines allow the overall responsiveness of this p53-binding site. The recognition sequence for p21 is shown in Figure 5D. This p53-binding site contains a low-redox potential guanine triplet in the complement strand, but the 5′ guanine is located at the interface the two half-sites, away from the contacting p53 residues in the major groove. Upon oxidation, an electron hole would preferentially localize to the 5′ location of the guanine triplet at the interface of the two half-sites, not in direct contact of p53, decreasing the likelihood of oxidation of each monomer and rendering the sequence nonresponsive.

These results allow us to make predictions regarding the responsiveness of other human p53 response elements to DNA CT. Of more than 200 known human p53-binding sites, we focused on sequences containing the canonical 5′-CWWT-3′ motif in both half-sites. An illustrative set of sequences, 21 about which we felt confident in making predictions, is provided in Table S1 of the Supporting Information.[42−45] Here, we highlight several interesting p53 response element predictions. Nonresponsive p53-binding sites include chromosome 12 open reading frame 5 (C12orf5) and matrix metallopeptidase 2 (MMP2).[46,47] For both of these genes, p53 serves as an activator. Under oxidative stress conditions, we predict p53 binding should not be affected by DNA CT and there should be no significant change in the regulation of that gene. C12orf5 will continue to be promoted, directing the glycolysis pathway into the pentose phosphate shunt while also protecting the cell from reactive oxygen species.[46] MMP2, also predicted to be nonresponsive, is involved in the breakdown of the extracellular matrix, which is useful for apoptotic processes.[47] In contrast, responsive p53-binding sequences that have been found include damage-specific DNA-binding protein 2 (DDB2), polo-like kinase 2 (PLK2), and protein phosphatase, Mg^{2+}/Mn^{2+}-dependent, 1J (PPM1J).[48−50] In all of these cases, p53 binding promotes the expression of these genes. As these sequences appear to be responsive on the basis of the purine pattern, we predict p53 oxidative dissociation by DNA CT, which will decrease the p53 occupancy and cause an overall downregulation of these gene products. DDB2 is necessary for the repair of DNA damage induced by ultraviolet light within the nucleotide excision repair pathway.[48] PLK2 is a member of the polo family of serine/threonine protein kinases, plays a primary role in normal cell division, and is necessary for the G1 to S transition.[49] PPM1J encodes a serine/threonine protein phosphatase of unknown overall function.[50] In all of these cases, oxidation should lead to downregulation, leading to lowered MMR pathway activity and tuning of cell cycle control. It should also be noted that a trend appears that nonresponsive promoter sequences controlling apoptosis-related gene products may be defended against oxidative damage. On the other hand, responsive promoter sequences controlling cell cycling and other pathways are not protected from oxidative damage because of their low-redox potential components.

The pattern and location of bases in the p53-binding site have been shown to play a critical role in how p53 may regulate the expression of different genes under oxidative stress conditions. DNA sequences with triplet guanine sites that make contact with p53 protein-binding sites are particularly prone to activating oxidation of the bound protein under oxidative stress conditions. This protein oxidation offers another layer of regulatory control and means of modifying specific proteins post-translationally to respond to an environmental signal. The fact that this modification can occur from a distance through DNA CT is more powerful still in permitting a host of regulatory effects on the genome that respond specifically and chemically to the guanine radicals generated with oxidative stress. Indeed, these results illustrate another unique role to consider for long-range CT within the cell.

■ ASSOCIATED CONTENT

Supporting Information

A representative EMSA of a p53′ serial dilution to determine the K_D of the protein with respect to AQ-conjugated oligonucleotides (Figure S1), representative guanine oxidation autoradiograms of each synthetic consensus sequence with p53′ (Figure S2), predicted responsive promoter sequences for oxidative dissociation of p53 (only p53 response elements composed of a canonical consensus sequence are included in these predictions, and the predicted p53 response to DNA CT is based upon the guanine pattern within the purine regions of each quarter-site) (Table S1). This material is available free of charge via the Internet at http://pubs.acs.org.

■ AUTHOR INFORMATION

Corresponding Author

*E-mail: jkbarton@caltech.edu. Phone: (626) 395-6075.

Funding

This work was supported by the Ellison Foundation (AG-SS-2079-08) and the Moore Foundation Center for Chemical Signaling.

Notes

The authors declare no competing financial interest.

■ ACKNOWLEDGMENTS

We thank Wendy M. Geil for assistance in the early stages of this project.

■ ABBREVIATIONS

p53′, full-length human p53 with stabilizing mutations M133L, V203A, and N268D; AQ, anthraquinone; CT, charge transport; LC, light control; R, purine; Y, pyrimidine; W, adenine or thymine.

■ REFERENCES

(1) Vogelstein, B., Lane, D., and Levine, A. J. (2000) Surfing the p53 network. *Nature 408*, 307−310.
(2) Vousden, K. H., and Lu, X. (2002) Live or let die: The cell's response to p53. *Nat. Rev. Cancer 2*, 594−604.
(3) Prives, C., and Hall, P. A. (1999) The p53 pathway. *J. Pathol. 187*, 112−126.
(4) Brooks, C. L., and Gu, W. (2006) p53 ubiquitination: Mdm2 and beyond. *Mol. Cell 21*, 307−315.
(5) El-Deiry, W. S., Tokino, T., Velculescu, V. E., Levy, D. B., Parsons, R., Trent, J. M., Lin, D., Mercer, W. E., Kinzler, K. W., and Vogelstein, B. (1993) Waf1, a potential mediator of p53 tumor suppression. *Cell 75*, 817−825.
(6) Kastan, M., Zhan, Q., El-Deiry, W. S., Carrier, F., Jacks, T., Walsh, W. V., Plunkett, B. S., Vogelstein, B., and Fornace, A. (1992) A mammalian-call cycle checkpoint pathway utilizing p53 and GADD45 is defective in ataxia-telangiectasia. *Cell 71*, 587−597.
(7) Joerger, A. C., and Fersht, A. R. (2007) Structure-function-rescue: The diverse nature of common p53 cancer mutants. *Oncogene 26*, 2226−2242.
(8) Paveletich, N. P., Chambers, K. A., and Pabo, C. O. (1993) The DNA-binding domain of p53 contains the four conserved regions and the major mutation hot spots. *Genes Dev. 7*, 2256−2564.
(9) Delaney, S., and Barton, J. K. (2003) Long-range DNA charge transport. *J. Org. Chem. 68*, 6475−6483.
(10) Genereux, J., Boal, A., and Barton, J. K. (2010) DNA-mediated charge transport in redox sensing and signaling. *J. Am. Chem. Soc. 132*, 891−905.
(11) Hall, D., Holmlin, R., and Barton, J. K. (1996) Oxidative DNA damage through long-range electron transfer. *Nature 382*, 731−735.
(12) Nunez, M. E., Hall, D. B., and Barton, J. K. (1999) Long-range oxidative damage to DNA: Effects of distance and sequence. *Chem. Biol. 6*, 85−97.
(13) Kelley, S. O., Holmlin, R. E., Stemp, E. D. A., and Barton, J. K. (1997) Photoinduced electron transfer in ethidium-modified DNA duplexes: Dependence on distance and base stacking. *J. Am. Chem. Soc. 119*, 9861−9870.
(14) Boon, E., Ceres, D., Drummond, T., Hill, M., and Barton, J. K. (2000) Mutation detection by electrocatalysis at DNA-modified electrodes. *Nat. Biotechnol. 18*, 1096−1100.
(15) Boon, E., Salas, J., and Barton, J. K. (2002) An electrical probe of protein-DNA interactions on DNA-modified surfaces. *Nat. Biotechnol. 20*, 282−286.
(16) Henderson, P. T., Jones, D., Hampikian, G., Kan, Y. Z., and Schuster, G. B. (1999) Long-distance charge transport in duplex DNA: The phonon-assisted polaron-like hopping mechanism. *Proc. Natl. Acad. Sci. U.S.A. 96*, 8353−8358.
(17) Slinker, J., Muren, N., Renfew, S. E., and Barton, J. K. (2011) DNA charge transport over 34 nm. *Nat. Chem. 3*, 228−233.
(18) Sugiyama, H., and Saito, I. (1996) Theoretical studies of GG-specific photocleavage of DNA via electron transfer: Significant lowering of ionization potential and 5′-localization of HOMO of stacked GG bases in B-form DNA. *J. Am. Chem. Soc. 118*, 7063−7068.
(19) Burrows, C. J. (2009) Surviving an oxygen atmosphere: DNA damage and repair. *ACS Symp. Ser. 2009*, 147−156.
(20) Kurbanyan, K., Nguyen, K., To, P., Rivas, E., Lueras, A., Kosinski, C., Steryo, M., González, A., Mah, D., and Stemp, E. D. A. (2003) DNA-protein cross-linking via guanine oxidation: Dependence upon protein and photosensitizer. *Biochemistry 42*, 10269−10281.
(21) Nunez, M. E., Holmquist, G. P., and Barton, J. K. (2001) Evidence for DNA charge transport in the nucleus. *Biochemistry 40*, 12465−12471.
(22) Nunez, M. E., Noyes, K. T., and Barton, J. K. (2002) Oxidative charge transport through DNA in nucleosome core particles. *Chem. Biol. 9*, 403−415.
(23) Merino, E. J., Boal, A. K., and Barton, J. K. (2008) Biological contexts for DNA charge transport chemistry. *Curr. Opin. Chem. Biol. 12*, 229−237.
(24) Sontz, P. A., Muren, N. B., and Barton, J. K. (2012) DNA charge transport for sensing and signaling. *Acc. Chem. Res. 45*, 1792−1800.
(25) Takada, T., and Barton, J. K. (2005) DNA charge transport leading to disulfide bond formation. *J. Am. Chem. Soc. 127*, 12204−12205.
(26) Gorodetsky, A. A., and Barton, J. K. (2007) DNA-mediated electrochemistry of disulfides on graphite. *J. Am. Chem. Soc. 129*, 6074−6075.
(27) Cho, Y., Gorina, S., Jeffrey, P. D., and Pavletich, N. P. (1994) Crystal-structure of a p53 tumor-suppressor DNA complex: Understanding tumorigenic mutations. *Science 265*, 346−354.
(28) Augustyn, K., Merino, E., and Barton, J. K. (2007) A role for DNA-mediated charge transport in regulating p53: Oxidation of the DNA-bound protein from a distance. *Proc. Natl. Acad. Sci. U.S.A. 104*, 18907−18912.
(29) Chen, Y., Dey, R., and Chen, L. (2010) Crystal structure of the p53 core domain bound to a full consensus site as a self-assembled tetramer. *Structure 18*, 246−256.
(30) Armitage, B., Yu, C., Devadoss, C., and Schuster, G. B. (1994) Cationic anthraquinone derivatives as catalytic DNA photonucleases: Mechanisms for DNA-damage and quinone recycling. *J. Am. Chem. Soc. 116*, 9847−9859.
(31) Gasper, S. M., and Schuster, G. B. (1997) Intramolecular photoinduced electron transfer to anthraquinones linked to duplex DNA: The effect of gaps and traps on long-range radical cation migration. *J. Am. Chem. Soc. 119*, 12762−12771.
(32) Nikolova, P. V., Henckel, J., Lane, D. P., and Fersht, A. R. (1998) Semirational design of active tumor suppressor p53 DNA binding domain with enhanced stability. *Proc. Natl. Acad. Sci. U.S.A. 95*, 14675−14680.
(33) Vallejo, A. N., Pogulls, R. J., and Pease, L. R. (2008) PCR mutagenesis by overlap extension and gene SOE. *Cold Spring Harbor Protoc.*, DOI: 10.1101/pdb.prot4861.
(34) Veprintsev, D. B., Freund, S. M., Andreeva, A., Rutledge, S. E., Tidow, H., Cañadillas, J. M., Blair, C. M., and Fersht, A. R. (2006) Core domain interactions in full-length p53 in solution. *Proc. Natl. Acad. Sci. U.S.A. 103*, 2115−2119.
(35) Zeglis, B. M., and Barton, J. K. (2007) DNA base mismatch detection with bulky rhodium intercalators: Synthesis and applications. *Nat. Protoc. 2*, 357−371.
(36) Maxam, A. M., and Gilbert, W. (1977) A new method for sequencing DNA. *Proc. Natl. Acad. Sci. U.S.A. 74*, 560−564.
(37) El-Deiry, W. S., Kern, S. E., Pietenpol, J. A., Kinzler, K. W., and Vogelstein, B. (1992) Definition of a consensus binding-site for p53. *Nat. Genet. 1*, 45−49.
(38) Saito, I., Nakamura, T., Nakatani, K., Yoshioka, Y., Yamaguchi, K., and Sugiyama, H. (1998) Mapping of the hot spots for DNA damage by one-electron oxidation: Efficacy of GG doublets and GGG triplets as a trap in long-range hole migration. *J. Am. Chem. Soc. 120*, 12686−12687.
(39) Gupta, S., Radha, V., Furukawa, Y., and Swarup, G. (2001) Direct transcriptional activation of human Caspase-1 by tumor suppressor p53. *J. Biol. Chem. 276*, 10585−10588.
(40) Wicki, R., Franz, C., Scholl, F. A., Heizmann, C. W., and Schäfer, B. W. (1997) Repression of the candidate tumor suppressor gene S100A2 in breast cancer is mediated by site-specific hypermethylation. *Cell Calcium 22*, 243−254.

(41) Cao, L. Y., Yin, Y., Li, H., Jiang, Y., and Zhang, H. F. (2009) Expression and clinical significance of S100A2 and p63 in esophageal carcinoma. *World J. Gastroenterol. 15*, 4183−4188.
(42) Riley, T., Sontag, E., Chen, P., and Levine, A. (2008) Transcriptional control of human p53-regulated genes. *Nat. Rev. Mol. Cell Biol. 9*, 402−412.
(43) Wei, C. L., Wu, Q., Vega, V. B., Chiu, K. P., Ng, P., Zhang, T., Shahab, A., Yong, H. C., Fu, Y., Weng, Z., Liu, J., Zhao, X. D., Chew, J. L., Lee, Y. L., Kuznetsov, V. A., Sung, W. K., Miller, L. D., Lim, B., Liu, E. T., Yu, Q., Ng, H. H., and Ruan, Y. (2006) A global map of p53 transcription-factor binding sites in the human genome. *Cell 124*, 207−219.
(44) Geer, L. Y., Marchler-Bauer, A., Geer, R. C., Han, L., He, J., He, S., Liu, C., Shi, W., and Bryant, S. H. (2010) The NCBI BioSystems database. *Nucleic Acids Res.*, D492−D496.
(45) Wilson, D., Charoensawan, V., Kummerfeld, S., and Teichmann, S. (2008) DBD—taxonomically broad transcription factor predictions: New content and functionality. *Nucleic Acids Res. 36*, D88−D92.
(46) Madan, E., Gogna, R., Bhatt, M., Pati, U., Kuppusamy, P., and Mahdi, A. (2011) Regulation of glucose metabolism by p53: Emerging new roles for the tumor suppressor. *Oncotarget 2*, 948−957.
(47) Werb, Z. (1997) ECM and cell surface proteolysis: Regulating cellular ecology. *Cell 91*, 439−442.
(48) Sun, N. K., Kamarajan, P., Huang, H., and Chao, C. (2002) Restoration of UV sensitivity in UV-resistant HeLa cells by antisense-mediated depletion of damaged DNA-binding protein 2 (DDB2). *FEBS Lett. 512*, 168−172.
(49) Burns, T., Fei, O., Scata, K., Dicker, D., and El-Deiry, W. (2003) Silencing of the novel p53 target gene Snk/Plk2 leads to mitotic catastrophe in paclitaxel (taxol)-exposed cells. *Mol. Cell. Biol. 23*, 5556−5571.
(50) Zolnierowicz, S. (2000) Type 2A protein phosphatase, the complex regulator of numerous signaling pathways. *Biochem. Pharmacol. 60*, 1225−1235.